

BackFi: High Throughput WiFi Backscatter

Dinesh Bharadia[†], Kiran Joshi[†], Manikanta Kotaru, Sachin Katti

Stanford University

{dineshb, krjoshi, mkotaru, skatti}@stanford.edu

[†]co-primary authors

ABSTRACT

We present BackFi, a novel communication system that enables high throughput, long range communication between very low power backscatter IoT sensors and WiFi APs using ambient WiFi transmissions as the excitation signal. Specifically, we show that it is possible to design IoT sensors and WiFi APs such that the WiFi AP in the process of transmitting data to normal WiFi clients can decode backscatter signals which the IoT sensors generate by modulating information on to the ambient WiFi transmission. We show via prototypes and experiments that it is possible to achieve communication rates of up to 5 Mbps at a range of 1 m and 1 Mbps at a range of 5 meters. Such performance is an order to three orders of magnitude better than the best known prior WiFi backscatter system [27, 25]. BackFi design is energy efficient, as it relies on backscattering alone and needs insignificant power, hence the energy consumed per bit is small.

CCS Concepts

•Information systems → Sensor networks; •Hardware → Digital signal processing; Sensors and actuators; Wireless integrated network sensors;

Keywords: Full Duplex Backscatter; Backscatter Communication; Internet of Things (IoT); WiFi Backscatter; Backscatter Decoder; Ambient Backscatter

1. INTRODUCTION

Embedded and connected gadgets - colloquially referred to as the Internet-of-things (IoT) - are increasingly making it possible to continuously monitor our bodies, personal lives and surroundings to improve health, energy usage, security and so on. These gadgets (e.g. wearable, fitness/health trackers, security cameras/microphones, thermostats [35]) integrate with cheaply available sensing technology to continuously measure physical variables such as temperature, heart rate, ambient sounds, etc. and upload them via wireless links

Permission to make digital or hard copies of all or part of this work for personal or classroom use is granted without fee provided that copies are not made or distributed for profit or commercial advantage and that copies bear this notice and the full citation on the first page. Copyrights for components of this work owned by others than the author(s) must be honored. Abstracting with credit is permitted. To copy otherwise, or republish, to post on servers or to redistribute to lists, requires prior specific permission and/or a fee. Request permissions from permissions@acm.org.

SIGCOMM '15, August 17 - 21, 2015, London, United Kingdom

© 2015 Copyright held by the owner/author(s). Publication rights licensed to ACM. ISBN 978-1-4503-3542-3/15/08...\$15.00

DOI: <http://dx.doi.org/10.1145/2785956.2787490>

to the cloud. Analytics applications then analyze such data to implement useful functionality such as fitness monitoring, intruder detection, regulating HVAC, etc. The future is likely to bring many more such devices helping us instrument more parts of our lives and surroundings, and enable us to measure and analyze almost every aspect of our lives.

We will refer to these IoT gadgets as either IoT sensors, or tags, or simply sensors in the remaining of our paper depending on the context. To widely realize the IoT vision, we believe that the wireless connectivity on these devices needs to satisfy three key requirements:

- **R1: Sufficient throughput & range:** A typical such gadget produces anywhere between a few Kbps (e.g. temperature sensors measuring every 100 ms) to a few Mbps (e.g., security microphones/cameras recording audio/video), and can be placed anywhere in the home or on the body. So the wireless link from the gadget to the wired gateway connected to the Internet should provide at least a *few Mbps of uplink throughput and 1-5 meters of range*.
- **R2: Very low power design:** These gadgets need to be able to operate for a long time without requiring battery replacements, or ideally without batteries at all. Recent work has demonstrated the possibility of powering these devices primarily using power harvesting from ambient RF sources such as TV and cellular signals. A typical RF powered device can harvest upto 100 microwatts of power [51, 44, 29] from TV signals. Hence, ideally the gadget's radio should provide the necessary throughput and range using a *few tens of microwatts of power* to be operable without batteries. If feasible this would eliminate the need for dedicated powering infrastructure such as RFID readers.
- **R3: Reuse ambient signals:** Ideally the IoT sensors should be able to piggyback their data on ambient, widely prevalent communication signals such as WiFi, Bluetooth etc. For example, while a WiFi AP is transmitting a packet to a standard WiFi client, an IoT sensor should be able to modulate its own information on the ambient WiFi signal and communicate its own data back to the AP. However this should not interfere with the normal WiFi communication from the AP to the client. If such a capability is feasible, then one can imagine being able to provide connectivity to IoT sensors using infrastructure that is already being widely deployed for standard wireless communication, thus reducing complexity and cost.

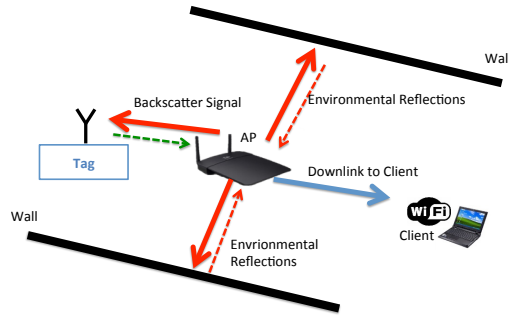


Figure 1: Overview of BackFi backscatter system : The AP transmits packet that is meant for the WiFi client (in blue), the transmitted signal (in red) is also reflected by reflectors in the environments like walls. The IoT sensor also receives these transmissions, and modulates its data on it and backscatters the signal to the AP (in green).

To the best of our knowledge, no current systems satisfies all three requirements. Recent work on WiFi backscatter [27, 25] is the closest, but it does not satisfy **R1**, it only provides around 0.5 Kbps of uplink-throughput and a range of 1 meter which is insufficient for many applications. RFID-based systems satisfy **R1** [55, 19, 49] and some of them satisfy **R2**, but not **R3**. They would require the widespread deployment of dedicated RFID reader infrastructure as well as require their own spectrum band of operation in the unlicensed band. Standard communication radios such as WiFi or Blue-tooth Low Power would satisfy **R1** and **R3**, but clearly cannot satisfy **R2**, they require between 30 – 50 mW (Blue-tooth) to several hundred mW (WiFi) of power to operate.

Our goal is to design a radio uplink for IoT sensors that satisfies all the above requirements. We present BackFi, a novel communication link design between backscatter IoT sensors and WiFi radios. The key contributions are a IoT sensor design for backscattering WiFi signals, and a novel radio circuit and algorithm design at the WiFi AP which doubles up as the (AP) reader decoding the backscatter signals from the IoT sensor. The AP reader operates while it is sending a standard WiFi packet to a standard WiFi client as seen in Fig. 1. The design satisfies the throughput and range requirements described above, it delivers at least 1 Mbps of throughput even at a range of 5m and much higher throughputs upto 6.67 Mbps at shorter ranges of a meter. To put these performance numbers in context, they are between one to three orders of magnitude better than the best known WiFi backscatter system [27, 25].

BackFi’s design makes three key technical contributions:

- First, we design a novel low power IoT sensor that can backscatter standard WiFi signals while being able to sustain high data rates of around 5 Mbps. The IoT sensor consists of a low power design for phase modulations ranging from BPSK to 16-PSK as well as mechanism for detecting WiFi transmission on which IoT sensor data can be modulated and backscattered.
- Second, a novel design of the WiFi AP radio such that it can receive the backscatter signals even while it is simultaneously transmitting a WiFi packet to a standard WiFi client. We leverage recent work on self-interference can-

celation for full-duplex radios to enable the backscatter signal to be received while the WiFi device is transmitting [17, 20, 43, 12, 8, 11, 9, 8, 26, 16, 39, 10]. Specifically, the backscatter signal is a modulated version of the transmitted signal itself. Hence self-interference cancellation has to be modified to ensure that the backscatter signal itself does not get canceled. We design novel self-interference estimation techniques that protect the backscatter signal from any degradation due to cancellation.

- Third, we invent novel demodulation and decoding algorithms that can estimate fine-grained changes in the backscatter signal to decode the IoT sensor data. Specifically, we show that WiFi backscatter can be modeled as a channel that is linear but time-varying modifying the IoT sensor data. BackFi incorporates novel decoding algorithms that can continuously track the time-varying channel and use standard diversity combining techniques such as Maximal Ratio Combining (MRC) to deliver a reliable, high throughput link [13].

We prototype BackFi and show that it can provide 5 Mbps of throughput at 1 m range and at least 1 Mbps at 5 m range. In comparison the best performing prior WiFi backscatter system [27, 25] provides a throughput of up to 1 Kbps, a range of less than a meter. We also show that BackFi has minimal impact on the operation of the standard WiFi network whose ambient signals it is piggybacking on to backscatter its own data.

We also note that the focus of this paper is on the uplink from the IoT sensor to the BackFi AP. The reason is that the IoT applications that we are designing for are bottle-necked on the uplink. These gadgets (such as fitness trackers, home sensors, wearables, etc) are collecting a lot of sensor data and need to upload them to the cloud and downlink often isn’t needed, or if it is, very low throughput of a few Kbps suffice [35, 53]. Hence in the rest of the paper we will focus on the uplink, but note that prior work has already demonstrated WiFi backscatter designs (which can be used with BackFi too) for the downlink that can provide upto 20 Kbps [27]. We further note that although we have chosen WiFi signaling for the description and implementation of BackFi, the system is applicable for other types of communication signals like Bluetooth, Zigbee, etc., as well.

2. RELATED WORK

BackFi is most closely related to recent work on WiFi backscatter [27, 25]. The prior design also uses ambient WiFi transmissions to backscatter data. Specifically, IoT sensors encode data in binary decisions of whether or not to backscatter the received packet transmission which is detected as changes in RSSI/CSI at a nearby helper WiFi device that is also receiving the packet from the AP. The design needs a helper device because the prior design doesn’t have self-interference cancellation, hence the transmitting AP cannot detect changes in RSSI/CSI while it is transmitting due to large self-interference. Since information is encoded in binary decisions that span an entire packet, the information rate is only 1 bit per WiFi packet. The range is

also low (less than a meter) because the WiFi helper needs the IoT sensors to be close to detect changes in RSSI/CSI. The reason is that the helper device needs to detect the changes in RSSI/CSI while it is receiving the strong WiFi transmission from the AP. This WiFi transmission essentially acts as interference to the detection of weak changes in RSSI/CSI induced by the tag's decision to backscatter or not, and thus limits range.

BackFi on the other hand does not have any of these limitations. Because it modulates information by changing the phase of the received WiFi signal at a much faster rate throughout the WiFi packet, it achieves three orders of magnitude higher throughput. Its range is an order of magnitude higher because self-interference cancellation enables the reader to completely clean out the effect of the ambient WiFi transmission and detect fine-grained changes in the backscatter signal. Finally BackFi provides a framework to analyze energy/bit, which is independent of platform (FPGA, ASIC, discrete) and the technology choice for implementation. However we note that the prior WiFi-backscatter system required no changes to the WiFi AP. BackFi does require the addition of self-interference cancellation hardware. So the trade-off is increased hardware complexity for a much higher throughput and range.

BackFi is related to a large body of work on RFID systems [19, 55, 50, 49, 23, 22, 52, 46, 45, 54, 14, 3], which use dedicated, powered reader infrastructure to supply power as well as receive data from the RFID IoT sensors [30]. The IoT sensors themselves are designed to be low power and may or may not have batteries. However the cost of deploying and maintaining dedicated reader infrastructure has tempered the adoption of these systems. BackFi and other WiFi backscatter systems [27] use ambient WiFi signals for communicating backscatter data, hence deployment is easier.

BackFi is also related to recent work on ambient backscatter communication [28, 34] that enables two RF powered devices to communicate with each other. However these systems do not provide connectivity to the Internet which is BackFi's primary focus. BackFi is also related but complementary to recent work on harvesting power from RF sources such as TV signals [28, 48, 30], cellular transmissions [33] and WiFi [27, 21, 25, 32]. These systems have demonstrated the ability to harvest around 60 – 100 μ W from ambient sources such as TV signals [46, 51, 44, 29] which is sufficient power to provide a high throughput battery-less IoT sensor. Hence with BackFi's high throughput, long range, and low power WiFi backscatter connectivity combined with the ability to harvest power from ubiquitous RF sources, we believe we are closer to the vision of RF powered, battery-less IoT sensors ubiquitously deployed and connected to the Internet.

BackFi advances the state-of-the-art in backscatter communication by being able to provide the following:

Improved backscatter decoder: BackFi's decoder presents a first formal framework to decode backscatter on wide-band signals. All the prior backscatter systems use tone as the excitation signals, whereas BackFi uses wideband signals. Further this framework can improve the decoding of the tone

based backscatter systems too. The reason is that the silent mode of BackFi eliminates all the backscattered signal by the rest of the environment (including the structural mode of antenna). This allows use of the information on the tone (excitation signal) for decoding, instead of nulling it as in most RFID decoders.

Effective backscatter protocol: BackFi presents a protocol for backscatter devices which allows an efficient decoding for backscatter system. For high order modulation, this design choice becomes imperative to provide good throughput and SNR.

Spectral Efficiency: BackFi presents a high throughput system by piggybacking on the existing data signaling like WiFi or Bluetooth. BackFi capability to reuse existing signaling makes it spectrally efficient and easy to seamlessly deploy. Moreover, since WiFi can be deployed in 900 MHz band too, deploying BackFi is much more effective than deploying RFID readers.

3. OVERVIEW

BackFi's basic mode of operation is shown in Fig. 1. A BackFi capable WiFi AP transmits a WiFi packet to a standard WiFi client. The IoT device with the BackFi tag backscatters the WiFi transmission back to the WiFi AP, and modulates its data on the backscatter signal. The AP decodes the backscatter signal to recover the data from the IoT gadget.

At a high level, the above description also applies to a RFID reader and RFID tag. So why can't we just reuse the RFID design to build WiFi backscatter systems? We argue why but start with a brief primer on standard RFID backscatter first.

3.1 How does traditional RFID work?

In traditional RFID systems, communication happens by the reader first transmitting an excitation signal which is typically a single frequency tone (a sinusoid) in the 900 MHz band. The tag receives this excitation signal and then backscatters (reflects) it after appropriately modifying the phase of the excitation signal. The data that the tag wishes to transmit is modulated on these phase changes. The tag design at a conceptual level is very simple, it is an antenna connected to an array of switches which are turned on and off appropriately to control the phase of the reflected signal from the tag. The array of switches is controlled by logic that reads the information bits, and computes the on-off routine that needs to be implemented on the switch to create the phase difference that encodes the information bits. The backscattered signal is then received by the reader whose goal is then to demodulate the signal by first detecting the phase changes introduced by the tag and then recovering the original data. The design of the tag is fairly standard and is not the focus of this paper, we refer the reader to a large body of literature [49, 30] on the circuit level details of implementing tags.

It is useful to construct a model of the signal that the reader receives after the tag backscatters the signal. If $x(t)$ is the excitation signal transmitted by the reader, it undergoes four distortions before it arrives back at the reader again after reflections and backscatter. First, the signal gets reflected

by objects in the environment other than the RFID tag and arrives back at the reader, we model this environmental distortion as h_{env} . The other portion of the signal is the one that first goes to the tag, has its phase changed to modulate data, and then comes back to the reader, i.e., the backscatter signal. We represent the forward channel between the reader and tag as h_f , the phase modulation at the tag is simply a multiplication of the received signal by $e^{j\theta(t)}$ and the backward channel is represented by h_b . The phase $\theta(t)$ is changed at the tag according to the data that is being modulated, for example, if DQPSK is being used, the phase w.r.t. the previous symbols phase is shifted by the appropriate multiple of 90 degrees. Note that $\theta(t)$ is changing at the rate of the symbol period at the tag. So the overall signal received back at the reader is given by:

$$y_{rx}(t) = \underbrace{x(t) * h_{env}(t)}_{environment} + \underbrace{\{(x(t) * h_f(t)).e^{j\theta(t)}\} * h_b(t)}_{backscatter} \quad (1)$$

The goal for the reader of course is to estimate $\theta(t)$ and thus demodulate the tag data. As the above equation shows, there are two challenges in accomplishing that. First is the environmental term; it contains no useful information and therefore acts as interference. This self-interference (because its generated by the reader's own transmission) is likely quite strong relative to the backscatter signal because it consists of direct leakage from the reader's transmitter to the receiver as well as reflections from nearby objects. In many cases, the self-interference and the backscatter signal can be separated by more than the dynamic range of the reader's receiver chain, which would end up completely drowning the backscatter signal. Second, if the environmental interference can be eliminated, the challenge is to estimate h_f and h_b , and then given that we know $x(t)$ it is simple to recover $\theta(t)$ and demodulate the tag data. The above two challenges are true for any backscatter system, we describe how current RFID systems handle them and why we cannot use that design for BackFi next.

3.1.1 Decoding Standard RFID Backscatter

In standard RFID based backscatter, the excitation signal is a sinusoid. So $x(t)$ in the above equation is $e^{j\omega_c t}$, where $\omega_c = 2\pi f_c$ is angular frequency and f_c is the carrier frequency (typically in the 900MHz ISM band). This simple fact ends up making both the interference cancellation and demodulation problem easier.

First, self-interference cancellation is simple because with a tone as the excitation signal, the interference term $x(t) * h_{env}(t)$ is simplified to $H_{env}(\omega_c)e^{j\omega_c t}$, where $H_{env}(\omega_c)$ is the frequency domain channel response corresponding to $h_{env}(t)$ and is evaluated at the tone frequency ω_c . In other words the original excitation signal is modified by a single complex number, essentially a single attenuation value and a phase shift. This is a special property of sinusoidal inputs to LTI channels, convolution simply becomes multiplication with the frequency domain channel response's value at the tone's frequency for tone inputs. This simplification does not apply to wideband signals such as WiFi. Hence to implement in-

terference cancellation, all we need is a tunable phase shifter and attenuator, which is programmed dynamically to emulate $H_{env}(\omega_c)$. The cancellation circuit would get a copy of the transmitted excitation signal as input, pass it through the phase shifter and attenuator which have been tuned to $\angle H_{env}(\omega_c)$ and $|H_{env}(\omega_c)|$ respectively. Finally, the design subtracts it from the received signal at the reader to eliminate the self-interference. Note that this is a well known technique and is implemented in commercial readers today [15, 5].

Similarly, recovering $e^{j\theta(t)}$ becomes easy because $x(t)$ is a simple tone. To see why consider the following mathematical simplification after substituting $x(t)$ with a tone, $e^{j\omega_c t}$:

$$\{(x(t) * h_f(t))e^{j\theta(t)}\} * h_b(t) = H_f(\omega_c)\{e^{j\omega_c t}e^{j\theta(t)}\} * h_b(t)$$

Further simplification happens after down-conversion to baseband at the reader:

$$y_{tag}(t) = H_f(\omega_c)h_b(t) * e^{j\theta(t)}, \quad (2)$$

which is a standard decoding problem on a linear time invariant system with channel $H_f(\omega_c)h_b(t)$ and input $e^{j\theta(t)}$. Hence standard phase demodulation and decoding techniques [38] can be applied to recover the original phase modulated data.

3.2 Why can't we reuse the above design for BackFi?

The key difference between BackFi and conventional RFID backscatter is that BackFi aims to use standard WiFi signals as the excitation signal. So none of the above simplifications that came about because the excitation signal was a simple tone apply. In fact the self-interference cancellation and demodulation problems become significantly harder as we show below.

First, self-interference cancellation now has to eliminate a relatively wider band signal, not just a tone. The implication is that the self-interference cannot be modeled as a simple attenuation and phase shift applied to the original excitation signal. For WiFi signals that typically span 20-40 MHz or even more wider bandwidths, the frequency domain representation of the distortion introduced by the environment, h_{env} is quite frequency selective. The practical implication is that a simple cancellation circuit that uses a programmable attenuator and phase shifter is not enough to cancel, in fact we need more sophisticated designs that can model the attenuation and phase shifts that happen over the entire bandwidth of the WiFi signal. Hence the traditional reader design for eliminating self-interference doesn't apply.

Second, and more importantly, the decoding problem no longer reduces to a standard demodulation problem at the reader like it did with a tone. To see why, the reader is now trying to recover the phase $\theta(t)$ from the following received signal at the reader after down-conversion:

$$y_{tag}(t) = (e^{j\omega_c t}x(t) * h_f(t)).e^{j\theta(t)} * h_b(t) \quad (3)$$

The above equation represents a **time variant** channel that transports the input $e^{j\theta(t)}$ into the output $y_{tag}(t)$, and the information that we are trying to decode is buried inside this time variant channel. The reason the channel term is time

varying is because the WiFi signal $x(t)$ is also acting as a channel distortion that is modifying $e^{j\theta(t)}$. Consequently standard decoding techniques designed for linear time invariant systems cannot be applied.

The main contributions of this paper are the design of self-interference cancellation and decoding techniques that can work when WiFi signals are used for backscatter. We also describe how BackFi ensures that it does not interfere with standard WiFi communication which the WiFi signal was originally created for.

4. DESIGN

BackFi uses ambient WiFi transmissions that are being sent by a WiFi AP to a standard WiFi client as the excitation signal. The tag receives the WiFi signal, modulates data on the received WiFi signal, and backscatters the signal to the AP. The architectural design of the BackFi tag is shown in Fig. 2. IoT sensor consists of BackFi tag and a sensor populating the data in the tag data memory unit.

4.1 The BackFi Link Layer Protocol

First, we describe how a BackFi AP activates and gets a BackFi tag to backscatter information. The protocol proceeds in two stages as described below.

How is the tag activated?

Whenever a BackFi AP transmits, if it is willing to receive backscatter communication, it follows a special protocol before transmitting the WiFi packet. Specifically, like in prior work [27], it transmits a *CTS_to_SELF* packet to force other WiFi devices to keep silent. Next it transmits a series of short pulses to encode a pseudo-random preamble sequence. If the preamble bit is one, then a pulse is transmitted and if its zero, no pulse is transmitted. The preamble is 16 bits long and each bit period lasts for a $1 \mu s$. The preamble is meant to be the signal to the BackFi tag that the BackFi AP is willing to listen to backscatter transmissions. Note that a preamble can be unique to a particular BackFi tag that is connected to this BackFi AP and can be used to select which BackFi tag gets to backscatter at that instant. In such cases, a tag only backscatters when it detects the preamble meant for it.

A BackFi tag by default is in an energy saving sleep mode if it has no data to transmit. If it has sufficient data to transmit (potentially after a sensor has collected enough data), the tag wakes up and listens for its preamble from the BackFi AP. To listen and detect the preamble, the tag uses an energy efficient detector circuit. To build our preamble detector we leverage a large body of work done in low power wake up radio design [40, 18, 36, 37]. These detectors work at power consumption between $98 nW$ [40] to $7.5 \mu W$ [18], and can detect input signals with power between -41 dBm and -56 dBm . The design has an envelope detector, a peak finder, a set-threshold circuit and a comparator. The envelope detector removes the 2.4 GHz carrier frequency from the received signal and the peak detector detects and holds the peak amplitude of the received signal after envelope detection. The set-threshold circuit obtains the output of the peak detector and outputs half the amplitude as the threshold. Finally the comparator compares the signal after the output of the enve-

lope detector with the threshold and outputs one bit whenever the received signal is greater than the threshold value and a zero bit otherwise. The comparator outputs a bit decision every microsecond, corresponding to the bit period in the preamble. Finally digital logic on the BackFi tag correlates the detected 16-bit long sequence over sliding windows with the known preamble associated with that tag, and if there is a match it activates the rest of the backscatter circuitry to begin modulation of its data.

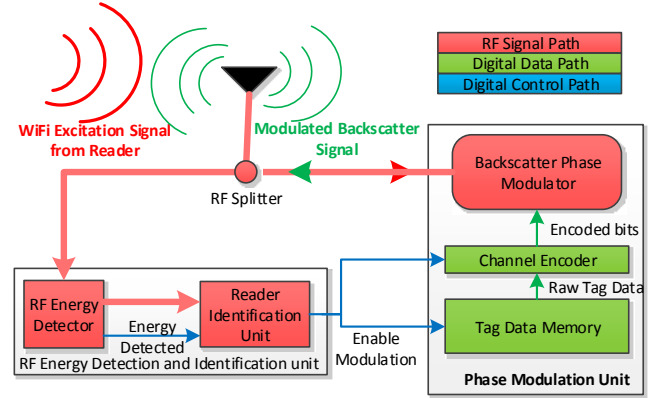


Figure 2: Architecture of the tag used in BackFi: Once the tag senses the WiFi excitation signal from the reader, it wakes up the modulation subsystem. The tag then reads the data to be uploaded and modulates it on the excitation signal by selecting discrete phase using the *Backscatter Phase Modulator*.

How does the tag modulate its data?

Fig. 4 shows the various timing events and packet format used by the BackFi tag. We will describe their functionality in detail later in this section, here we give a brief overview. Once the excitation energy is detected and the reader is identified (which lasts $16 \mu s$), the tag goes into a *silent period* that lasts for another $16 \mu s$. During this time the tag will suppress any backscatter transmission, which allows the reader to estimate the channels needed for self-interference cancellation as described in Sec. 4.2. After that the tag transmits its own *preamble* sequence for $32 \mu s$ that is known at the BackFi reader. Using this sequence the reader can estimate the channels it needs for decoding the backscatter data. This sequence is a pseudo random with very high auto-correlation, and is used by the reader to find the symbol timing from the tag.

The tag then sends its data payload by phase modulating the received signal. Specifically, let's say the tag is using QPSK modulation, hence there are four symbols $[e^{j\theta_1}, e^{j\theta_2}, e^{j\theta_3}, e^{j\theta_4}]$ in the constellation map separated by 90 degrees on which two bits of information can be modulated. The tag reads the data that needs to be transmitted, picks out two bits at a time, maps it to the appropriate QPSK symbol and then multiplies the received excitation signal from the WiFi transmitter with the corresponding phase signal, $e^{j\theta_i}$, $i = 1 \dots 4$ to modulate the data on to the WiFi signal. The specific circuit by which the phase modulation signal $e^{j\theta_i}$ is generated is a well studied problem and has been widely used in RFID

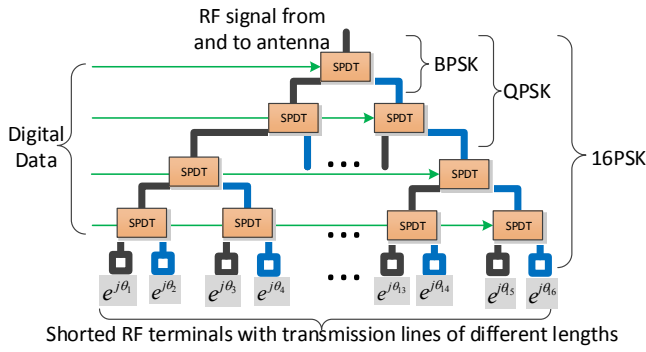


Figure 3: Structure of the backscatter phase modulator used in the tag of BackFi: The four digital signal can be used to select one of the 16 possible phases at the leaf of the tree. The incoming RF signal traverses from the top input port all the way to the selected leaf node and is reflected back from the short circuited terminals to the input RF port.

tags [49]. Fig. 3 shows the detail of the RF phase modulator we use in the BackFi tag.

The phase modulator consists of several RF Single Pole Double Throw (SPDT) switches that are connected in a binary tree structure. These switches can pass incoming RF signal to one of the two ports. These switches can be controlled using digital signals and the tag uses the data to be modulated as the control signal for these switches. At the leaf of the switch tree, different lengths of RF traces are connected. These trace lengths are designed specifically to achieve the discrete phase shift required for the supported constellation. The number of SPDT switches is determined by the number of constellation points that are supported. For example, for BPSK only one switch is needed, for QPSK three switches are needed and for 16-PSK 15 switches are needed. Also, if the tag can support higher modulations, then all the lower modulations can also be supported. For example, the design in Fig. 3 can support 16-PSK, QPSK, and BPSK, by appropriately preventing some of the switches from toggling as shown in the figure.

To improve the performance of the link the tag also employs simple channel encoding using convolutional codes. The convolutional codes are powerful error correcting codes yet their encoders are very easy to implement using few standard digital components which incurs small energy penalty on the tag. For example, a rate $\frac{1}{2}$ convolutional encoders with constraint length of 7, will require 6 shift registers and 8 XOR gates.

Tag Symbol Rate: The BackFi tag also has a choice on the rate at which it will generate the phase modulation symbols by controlling the switching frequencies on the SPDT switches. The trade-off here is that higher frequencies consume more power and energy, hence the actual rate to use is a function of how much energy is available either via batteries or harvesting. In BackFi tags, this is a configurable parameter ranging from 0.01 megasymbols/second (MSPS) to 2.5 MSPS.

Next, the BackFi AP after receiving the phase modulated, backscattered signal proceeds to decode the tag's data. As discussed in the previous section, the two key challenges

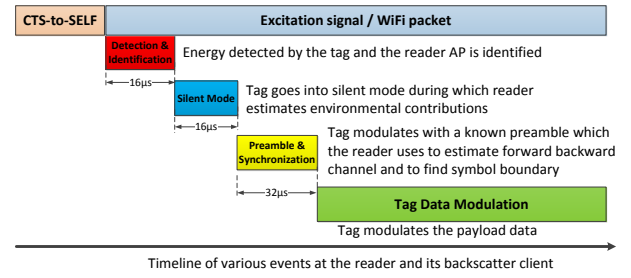


Figure 4: The BackFi AP first sends out the CTS-to-SELF to force other WiFi into silent mode. It then sends out the energy detection and identification data to its backscatter client. Once the WiFi excitation signal is received by the tag, it goes through sequence of operations shown above before modulating its data on the excitation signal. The excitation signal is in fact a WiFi packet meant for a regular WiFi client which receives and decodes the WiFi packet without ever noticing the presence of the backscatter communication that is happening simultaneously.

here are wideband self-interference cancellation and time-varying decoding. We describe how BackFi addresses these challenges next. Note that the channel model of the signal received back at the reader with BackFi is exactly the same as standard RFID backscatter and has been derived in Eq. 3, the only difference of course is that $x(t)$ is the WiFi OFDM signal instead of a tone.

4.2 Self-Interference Cancellation

Like conventional RFID systems, the tag's backscatter signal in BackFi is buried under strong self-interference. This interference stems from two sources: direct leakage from the AP's transmit chain to the receive chain and from reflections of the WiFi transmission by non-tag objects in the environment. But unlike the single tone excitation signal in RFID, BackFi's excitation signal is a wideband WiFi OFDM signal. Because of the wideband nature, scaling the excitation signal by a single attenuation and phase shift is not sufficient to model the self-interference. This is because different frequency components of the WiFi signal add constructively or destructively due to the multi-path effect which results in frequency dependent scaling and phase shifts. However, this problem has been studied extensively in recent years for designing full-duplex radios [12] where self-interference needs to be suppressed to be able to simultaneously listen to weak signals that are being received. The difference in BackFi from those scenarios is that the backscatter signal (which corresponds to the weak signal we want to receive) is a modified version of the transmitted signal, whereas in standard full duplex that is a completely independent signal originating from another sender. So BackFi leverages the recent work on full duplex, but modifies it appropriately to handle the fact that backscatter signals are highly correlated with the self-interference signal.

We briefly review the design of self-interference cancellation systems for completeness, but refer the reader to prior work [12] for a complete description. Self-interference cancellation systems first estimate the channel $h_{\text{env}}(t)$ that the leaked and reflected signal have gone through before reaching back at the receiver. This estimated channel distortion

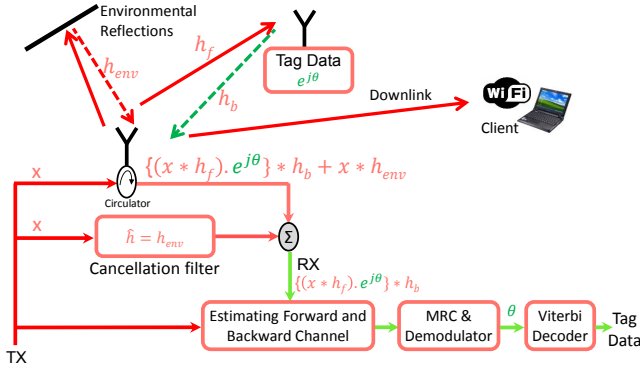


Figure 5: Architecture of the reader used in BackFi: The reader transmits the excitation signal x which is actually a WiFi packet meant for a client. This signal is reflected by the environment, which the reader cancels using *cancellation filter*. The residual signal after cancellation is used to estimate the forward and backward channel from and to the tag. The reader then applies MRC to estimate the tag data $\hat{\theta}$, which is further improved by passing it through Viterbi decoder.

is applied to a copy of the transmitted WiFi signal to recreate the self-interference accurately, and the distorted signal is then subtracted from the received signal to eliminate self-interference. The distortion application and subtraction happens in two stages, analog and digital. Analog cancellation is necessary to ensure that the receiver's ADC is not saturated by self-interference which would drown out the weak backscatter signal before being received in baseband. Analog cancellation is implemented using a combination of RF FIR filters and couplers [12], but cannot completely eliminate self-interference due to the imprecision of analog components. Hence a second digital cancellation stage is employed after the signal is sampled by the receiver's ADC to eliminate the residual self-interference. Digital cancellation is implemented via digital FIR filters. Fig. 5 shows the design.

If we directly apply the prior design, it will end up canceling parts of the backscatter signal too. The reason is that prior design aims to accurately estimate the non-linear transfer function that captures the relationship between the transmitted signal and the received signal [12]. But as we have shown in the previous section, the backscatter signal is actually a non-linear transformation of the transmitted signal. If naively applied, prior designs would end up canceling the backscatter signal too which would reduce the SNR and throughput of tag's transmissions back to the reader.

To tackle this, BackFi's link layer design ensures that during the channel estimation phase of self-interference cancellation, there is no backscatter transmission. Specifically, when a BackFi tag is excited by a WiFi transmission, they do not instantly start backscatter. Instead they employ a *silent period* of $16 \mu s$ as shown in Fig. 4, during which they do not backscatter, and only then start modulating their data on to the received signal and performing backscatter. We show experimentally that this small silent period is sufficient for the reader/AP to estimate the self-interference channel and perform cancellation for the rest of the WiFi packet. Since

there is no backscatter during the channel estimation phase, self-interference cancellation does not model the backscatter reflections and therefore they are not affected by cancellation.

At this stage, the reader/AP is left with just the non-linear backscatter reflection from the tag, and its goal is to decode the data. We describe this step next.

4.3 Decoder Design of BackFi

As reviewed before, since the WiFi signal $x(t)$ is wideband, the excitation signal received at the tag $z(t) = x(t) * h_f(t)$ cannot be considered as simple scaled and phase shifted version of $x(t)$ as with standard RFIDs. Hence after the removal of the self-interference, the residual signal at the reader after down-conversion to baseband is given by

$$y_{\text{tag}}(t) = \underbrace{\left[(x(t) * h_f(t)) e^{j\theta(t)} \right]}_{\text{tag signal}} * h_b(t). \quad (4)$$

Here, the signal $x(t)$ is the WiFi transmission that the reader is sending. This signal is wideband and varying but known to the reader. The channels h_f and h_b are the forward and the backward channels. These channels can be considered time invariant for the duration of the tag packet but are unknown. The goal is of course to recover the tag signal $e^{j\theta(t)}$ from the above equation. This is challenging because the tag signal is being modified by a time varying unknown channel, namely $x(t) * h_f(t)$. Contrast this with standard RFID decoding at the reader in Eq. 2, where the tag signal is being modified by a time-invariant channel since both $h_f(t)$ and $h_b(t)$ are time-invariant for the duration of the tag packet. We describe how BackFi tackles this time-varying decoding problem next.

4.3.1 Estimating the forward/backward channels

First, the BackFi AP estimates the forward and backward channels, $h_f(t)$ and $h_b(t)$. We can assume these channels to be time invariant for the duration of the tag packet, hence to estimate them we use a standard communication technique: a preamble. Specifically, after the tag detects that it should backscatter and stays quiet for the *silent period*, it modulates a constant phase $e^{j\theta_{pre}}$ on the backscatter signal for a fixed period of $32 \mu s$. Thus during the *preamble interval* the received tag signal at the reader is given by

$$y_{pre}(t) = x(t) * [h_f(t) * h_b(t)].$$

Now since $x(t)$ is known, this becomes a standard channel estimation problem encountered in every communication system. We omit the details of the channel estimation technique and refer the reader to the vast amount of literature on this topic [38]. The channel estimation algorithm thus calculates the value of $h_f(t) * h_b(t)$.

Note that the above procedure only provides an estimate of the combined forward-backward channel, but not the individual channels. Hence the decoding step has to work only with the combined channel estimate.

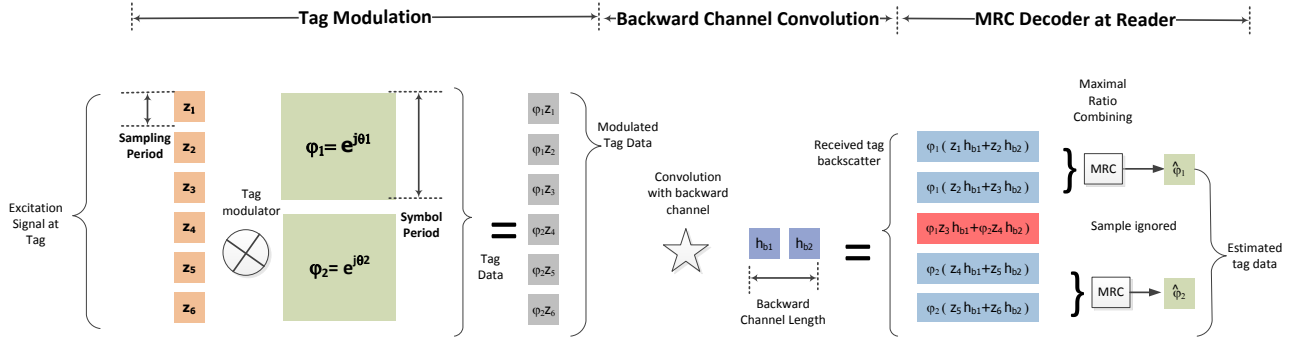


Figure 6: Discrete time representation of the design of BackFi: The samples of the WiFi excitation signal z is multiplied by the data ϕ at the tag. The modulated signal then passes through the backward channel h_b . The sampling period of WiFi is much smaller than the symbol period of the tag. This results in multiple copies of the tag data over several sampling period at the reader. These multiple copies are combined optimally by the MRC to estimate the tag data $\hat{\phi}$.

4.3.2 Decoding the Tag Data

The final step is decoding the tag data itself. BackFi's key insight here is the fact that symbol times for tag data are quite long due to the need to conserve energy at the tag. Specifically the tag modulates data by changing the phase term in $e^{j\theta(t)}$. Changing the phase is implemented by switching a transistor as described in Sec. 4.1. Transistor energy consumption scales linearly with switching frequency, hence tags use low rate switching frequencies. Typical transistor switching frequencies in tags are on the order of 0.5 – 2.5 MHz in tags, hence the symbol period in a tag is between 500 – 2000 ns. How can we exploit this insight to decode the data?

Our observation is that the delay spread in a typical channel between the reader and the tag is far smaller than 500 ns. In other words the length of the channel is far smaller. Intuitively this is because typical distances between a reader and a tag are around 10 m, so even accounting for reflections the extra multipath delay spread is small. Hence a channel usually lasts for 50 – 80 ns. But the symbol period from the tag is much longer at 500 ns, hence for the duration of the channel, we can consider the tag signal to be an unknown constant $e^{j\theta_c}$. BackFi leverages this insight to decode, it looks at the part of the symbol period (with some guard periods at the start and end of the symbol time as shown in Fig. 6 and tries to find the value of the constant phase within that period.

Specifically, with a constant phase from time $t_1 - t_2$, we can rewrite the decoding equation at the reader as:

$$y(t) = (x(t) * [h_f(t) * h_b(t)])e^{j\theta_c} + N; t_1 \leq t < t_2 \quad (5)$$

Note that all the terms except $e^{j\theta_c}$ are known in the above equation. A natural next step might be to divide $y(t)$ by $x(t) * [h_f(t) * h_b(t)]$ but this works poorly because it will also divide the noise term in the above equation and in many scenarios amplify it.

To tackle this, we turn to an old trick in communication theory: maximal ratio combining. To see how this works it helps to write the above equation in the discrete domain (the

representations are equivalent assuming sufficient sampling rate) as follows:

$$y_{\text{tag}}[n] = e^{j\theta[n]} \mathbf{x}_{n,L+M}^T \mathbf{h}_{fb} \quad \forall n \in [n_1, n_2] \quad (6)$$

Here L is the length of the forward channel, and M is the length of the backward channel. The \mathbf{h}_{fb} is the length $L + M$ vector of the combined forward-backward channel and $\mathbf{x}_{n,L+M} = [x_n \dots x_{n+L+M-1}]^T$ is a vector of length $L+M$ constructed using the excitation data $x[n]$, and we have assumed that the tag signal is constant for the period $[n_1, n_2]$. The above equation is simply a discrete version of Eq. 5 with the discrete convolution operation represented as dot product of vectors $\mathbf{x}_{n,L+M}$ and \mathbf{h}_{fb} .

Notice that the tag signal is expressed in terms of the forward-backward channel that we have estimated earlier, and therefore individual estimates of the forward and the backward channel are not needed. Also note that the tag modulation is constant for $n_2 - n_1 + 1$ interval which is larger than $L + M$, this is restating the same insight that length of the forward and backward channels is much smaller than the symbol period of the tag. So we will have $n_1 + n_2 - L_M$ different values of $y_{\text{tag}}[n]$ which contains information of the unknown but constant tag signal $e^{j\theta_c}$. We can leverage this fact to combine all these values to obtain the most likely value of θ_c that could have produced those sequence of observations of $y_{\text{tag}}[n]$ over the period $[n_1, n_2]$ using maximal ratio combining (essentially the same as temporal diversity combining). Specifically MRC would use the following formula to estimate θ_c ,

$$\hat{\theta}_c = \frac{\sum_{n=n_1}^{n_2} \hat{y}_{\text{tag}}[n]^G y_{\text{tag}}[n]}{\sum |\hat{y}_{\text{tag}}[n]|^2}, \quad (7)$$

where $\hat{y}_{\text{tag}}[n]$ is the expected tag backscatter signal without the modulation and can be computed as

$$\hat{y}_{\text{tag}}[n] = \mathbf{x}_{n,L+M}^T \mathbf{h}_{fb} \quad \forall n \in [n_1, n_2],$$

and G is the complex conjugate operator. Essentially the different measurements of y over that interval are weighted ap-

appropriately and combined to produce the most likely estimate of θ_c .

At this point, we have a robust estimate of the tag data for that symbol. The algorithm is repeated for all the symbols in the tag packet. There may still be decoding errors of the n-PSK symbols, which we can correct by using a standard channel code on top. In BackFi, we use a convolutional code at the tag to improve the link performance. The coding provides additional robustness and is decoded using a standard Viterbi decoder [38], we omit the details for brevity.

5. IMPLEMENTATION

We build a prototype of both the AP and tag of BackFi system. We describe their implementation details below.

5.1 BackFi AP

The BackFi AP is implemented using WARP software radios. The WARP incorporates a standard 20 MHz WiFi baseband operating in the 2.4 GHz range. We also use the same implementation on a WARP board to work as a WiFi client in our experiments. Further the decoding logic for backscatter signals is also implemented in the WARP FPGA [7]. For self-interference cancellation, we reproduce the recent design on single antenna cancellation [12, 11].

5.2 BackFi Tag

The IoT sensor is designed to operate across the 2.4 GHz WiFi channels. The prototype uses a 2.4 GHz omni-directional antenna that can receive and backscatter WiFi signals and has a gain of 3 dB. In our current prototype, logic implemented on a Kintex Kc705 board [6] supplies the data to be transmitted and configures the backscatter circuitry. This can be replaced with custom ASIC in a full design which would consume significantly lower energy.

The backscatter circuitry implements two components on the uplink: *the detector*, and *the modulator*. The modulator implements BPSK, QPSK and 16-PSK modulation. The phase modulation is implemented using SP4T switches. We chose phase modulation instead of n-QAM because this will result in the least amount of RF signal degradation during the backscatter modulation.

5.2.1 Energy consumption efficiency metric

In order to compare various implementation choices for IoT sensor, traditionally Energy per Bit (EPB) measured in average joules of energy required to transmit one bit of information has been used as a metric for energy efficiency. However, EPB varies significantly with the implementation platform. For example, the EPB for an IoT sensor implemented using off-the-shelf discrete components can be orders of magnitude larger than the EPB for IoT sensor implemented in a sub-micron ASIC design. Even for the sub-micron ASIC designs, EPB varies significantly depending on the technology node chosen (say 65-nm CMOS node vs 45-nm CMOS node) and the design choices (low power sub-threshold CMOS design vs traditional strong inversion CMOS design). BackFi's contribution is in showing how the EPB of an IoT sensor are related to each other for various communication parameters on a particular implementation platform.

For example, if an IoT sensor can choose BPSK or QPSK for communication, an interesting question may be, what is the relationship between the EPB of these two cases. While to the first order the EPB of these two cases should be the same and only the throughput should double going from BPSK to QPSK, a more detailed analysis shows that EPB is not the same for these two cases.

To understand why, let us refer to the architecture of the RF modulator as shown in Fig. 3. While BPSK requires only one SPDT switch, the QPSK requires three SPDT switches with double the throughput, therefore the EPB of the modulator goes up by a factor of $\frac{3}{2}$. Likewise, for 16-PSK we need 15 SPDT switches, but the data rate improvement is only 4 times compared to the BPSK, therefore the relative EPB for modulator increases by a factor of $\frac{15}{4}$. Also, power consumption in IoT sensor has two major components, the first one is dynamic power resulting from the charging and discharging of capacitors in various sub-systems of the IoT sensor as digital logic is computed, and the second is static power which is either due to leakage, or due to constant current required by some of the analog components in the IoT sensor. Because of the static power, the EPB is also affected by the symbol rate of the IoT sensor as the device takes longer time to transmit the same amount of data. For example, an IoT sensor can reduce the symbol rate which results in the improved SNR at the BackFi from MRC, but at the same time the static power consumption of the circuits will increase thereby increasing the overall EPB.

In order to show the energy efficiency trade-offs associated with the various choices offered by BackFi and to decouple them from the energy efficiency gained from actual choice of the implementation platform, we will present the remainder of the results using unit-less Relative Energy per Bit (REPB). We will first describe how energy consumption is modeled for our exemplary IoT sensor as shown in Fig. 2 and then show how we can compute its REPB for different parameter choices.

We have modeled the EPB of the tag by identifying the major power consumption modules of the IoT sensor architecture shown in Fig. 2. The three major contributors for EPB of this design are: *the RF modulator*, *the channel encoder* and *the memory*. As discussed earlier, the EPB of RF modulator varies depending on the chosen modulation index because the ratio of bit rate to the number of SPDT switches varies as we change the modulation index. In our current energy model we have computed the static and dynamic EPB of RF modulation unit by appropriately scaling the data provided for an industry standard modulator, the Analog Devices ADG904 [1].

BackFi uses a convolutional encoder to reduce bit error rates (BER). The exact EPB contributed by the encoder circuit is a very small fraction of the total EPB required for communication because convolutional encoders with moderate constraint length (7 in BackFi) require only 6 shift registers and a few XOR gates to encode the IoT sensor data. But the major EPB contribution comes from the coding rate associated with the convolutional encoder. For example, a $\frac{1}{2}$ rate code will essentially double the EPB of the RF mod-

ulator because the IoT sensor will transmit twice the actual amount of data on the channel. Likewise, a rate $\frac{2}{3}$ code will bump the RF modulator's EPB by a factor of $\frac{3}{2}$ and so on.

And finally BackFi also models the EPB associated with the memory read of the data in the IoT sensor. Because memory reads are performed for the sole purpose of backscattering the data to the BackFi's reader, we believe it is very important to include the read energy associated with the memory element as part of the overall EPB. In our current energy model we have computed the static and dynamic EPB of the memory read by using data provided for Cypress Semiconductor CY62146EV30 [2].

Using the above energy modeling technique we can now compute the EPB required for a particular choice of communication parameters: *channel code rate*, *symbol switching rate*, *modulation index*

$$\text{EPB} = \text{EPB}_{\text{mem}} + \text{EPB}_{\text{mod}} + \text{EPB}_{\text{enc}}. \quad (8)$$

Here EPB_{mem} is the EPB associated with the memory read inside the IoT sensor. This has two parts, the dynamic EPB that is dependent on the number of read operations per bit of data of IoT sensor, and the static part that is dependent on the symbol switching rate T_s ,

$$\text{EPB}_{\text{mem}} = \text{EPB}_{\text{mem,read}} + P_{\text{mem,static}} \times T_s.$$

Similarly, we can express the EPB associated with the convolutional encoder EPB_{enc} and the modulator EPB_{mod} with their constituent dynamic and static EPB.

In order to obtain the unit-less REPB, we use EPB for one set of such communication parameters as a reference and then divide the EPB for all the other choices with this reference EPB. In our current evaluation, we use $\frac{1}{2}$ rate code with BPSK modulation with symbol switching rate of 1 Mbps as reference communication parameters to compute the reference EPB. Based on the datasheets of the referred parts we computed the EPB for this reference case to be 3.15 pJ/bit.

Also, we have excluded the EPB associated with the energy detection logic as we believe their contribution to the overall EPB will be insignificant. The energy detector is based on prior work on wake up radio [40, 31]. The power consumption of this detector is around 100 nW. The energy detection needs to be done once for every backscatter packet and lasts for 16 μ s. A typical backscatter packet will have 1000 bits of information in it. Based on these information the EPB contributed by the detection logic is in femtojoules per bits which is practically negligible. The wake up radio can detect input signals as weak as -41 dBm, which provides sufficient range to wake up the tag radio even at a distance of 5 m from the AP. The same detection circuitry can be used to implement the downlink communication to the tag from the AP reader. The protocol for downlink communication has been described in prior work [27]. BackFi reuses this design for the downlink and provides similar throughputs of 20 Kbps. Since our focus in this work is on the up-link design we will evaluate it in detail in the next section by using REPB given by Fig. 8 as one of the metrics.

Symbol switching rate	Metric	BPSK, 1/2 rate	BPSK, 2/3 rate	QPSK, 1/2 rate	QPSK, 2/3 rate	16PSK, 1/2 rate	16PSK, 2/3 rate
10 KHz	REPB	29.2162	28.1984	31.2517	29.7250	40.4117	36.5951
	Thruput (Kbps)	5	6.67	10	13.33	20	26.66
100 KHz	REPB	3.5651	3.3333	4.0287	3.6810	6.1151	5.2458
	Thruput (Kbps)	50	66.7	100	133.3	200	266.6
500 KHz	REPB	1.2850	1.1231	1.6089	1.3660	3.0665	2.4592
	Thruput (Mbps)	.25	.33	.5	.67	1	1.33
1 MHz	REPB	1.0000	0.8468	1.3064	1.0766	2.6855	2.1109
	Thruput (Mbps)	.5	.67	1	1.33	2	2.67
2 MHz	REPB	0.8575	0.7086	1.1552	0.9319	2.4949	1.9367
	Thruput (Mbps)	1	1.33	2	2.67	4	5.33
2.5 MHz	REPB	0.8290	0.6810	1.1250	0.9030	2.4568	1.9019
	Thruput (Mbps)	1.25	1.67	2.5	3.33	5	6.67

Figure 7: Table provides BackFi tag's relative EPB and corresponding data rate for different choices of modulation, coding and tag symbol switching rate.

6. EVALUATION

We evaluate BackFi's design in an indoor environment in our lab with rich multi-path reflections and dense WiFi deployment. Our evaluation reveals the following:

- BackFi provides three orders of magnitude higher throughput, an order of magnitude higher range compared to the best known WiFi backscatter system [27, 25]. Specifically BackFi can provide a throughput of 5 Mbps at 1m range and a throughput of 1 Mbps at 5 m range from the BackFi AP.
- BackFi's throughput and range are comparable to traditional RFID platforms such as Ekhonet [55]. The key benefit of course is that BackFi is a WiFi back-scatter system and does not need dedicated reader infrastructure or frequency spectrum.
- BackFi has negligible (less than 5%) impact on the standard WiFi network's throughput even when the IoT sensor is concurrently backscattering WiFi signals.

6.1 Throughput, Range, and REPB

First, we evaluate the trade-off between throughput, distance, and REPB for BackFi. For any given distance, BackFi can deliver a set of throughputs by picking the appropriate combination of symbol switching rate, modulation, and coding rate. Each choice of symbol switching rate and modulation has a different throughput as well as different REPB as described in Section 5.2.1. Fig. 7 shows the REPB and throughput for every combination of symbol switching rate, modulation, and coding rate. The EPB for each of the these entries can be calculated simply by multiplying REPB and EPB of the reference parameters (BPSK, 1/2 rate with symbol switching rate of 1 MHz).

Note that while throughput monotonically increases from left to right in the table, REPB does not. For example, at an IoT sensor symbol switching rate of 1 MSPS, going from (QPSK, 1/2) to (QPSK, 2/3) results in a decrease in REPB. The reason is that energy needed to switch from 1/2 rate to 2/3 rate is not significant compared to the other energy contributions for this technology node and the increased throughput causes the REPB ratio to decrease. However, if at a certain range if the link SNR is such that both (QPSK, 1/2) and (QPSK, 2/3) encoded backscatter signals can be decoded at

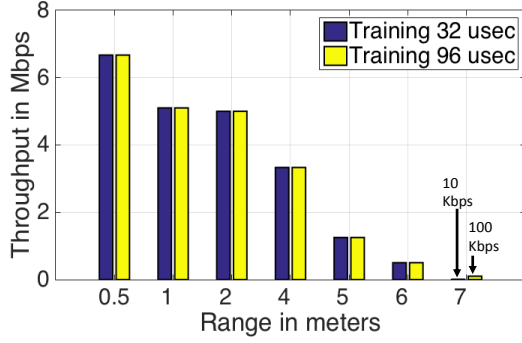


Figure 8: Relationship showing range of BackFi and maximum possible data rate possible for two different training times. At 7 meter, if we increase the preamble duration from 32 μ sec to 96 μ sec, it provides 10 \times improvement in the throughput.

the reader, then BackFi would never use (QPSK, 1/2). The rate adaptation algorithm would always pick the modulation, coding rate and symbol switching rate combination with the lowest REPB since the most precious resource here is energy, whether it comes from harvesting or batteries.

Next, we evaluate the throughput and range performance in our testbed. For these experiments we use our WARP based BackFi implementation for the BackFi AP to decode the IoT sensor's backscatter signals. The BackFi AP and the WiFi client are placed such that the maximum WiFi bit rate is 54 Mbps. They are configured to run on WiFi channel-6 in the 2.4 GHz range. The results for other WiFi channels are similar and not presented due to lack of space.

Impact of Range on Throughput: The BackFi's IoT sensor is placed at distances ranging from 0.5 m to 7 m. For each distance, we cycle the IoT sensor through all combinations of symbol switching rates and modulations, and then calculate throughput for combinations that can be decoded at the reader. In each iteration of the experiment, the BackFi's AP reader transmits 1 to 4 ms long packet at 24 Mbps bitrate including the backscatter start sequence as discussed in Sec. 4.1. The IoT sensor backscatters for the entire duration of the packet and stops when its detection logic signals the end of the transmission. We repeat the experiment 20 times at each combination of distance and BackFi throughput. Fig. 8 plots the maximum throughput achieved as a function of range for two different preamble duration of 32 μ s and 96 μ s.

Results: As we can see, BackFi is able to achieve a maximum throughput of around 6.67 Mbps at a distance of 50 cm. For more practical ranges, BackFi achieves a throughput of 1 Mbps at a distance of 5 m and around 5 Mbps at a distance of 1 m. This performance is three orders of magnitude better in throughput at the same range as compared to the best known WiFi backscatter system [27, 25]. Note, at 7 m the increased preamble duration of 96 μ s shows a 10 \times increase in the throughput. This is due to the fact that a shorter preamble results in an inaccurate estimate of the forward-backward channel which limits the SNR of the backscattered signal. Hence, for 32 μ s preamble, the IoT sensor compen-

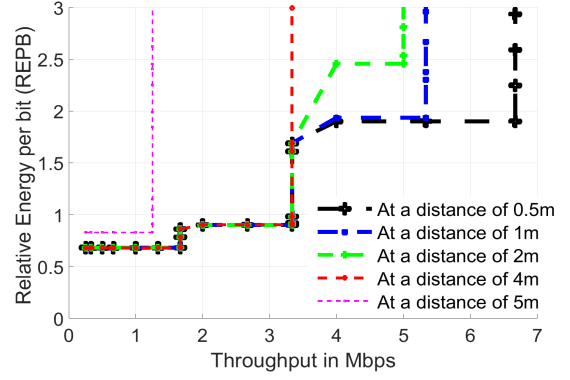


Figure 9: Each plot is BackFi's REPB for corresponding throughput achieved for the range varying between 0.5 m to 5 m. For example, we see that at a distance of 2 m to achieve 4 Mbps throughput we need to spend much more energy per bit than at a distance of 1m. Also, the vertical line indicates the maximum throughput that is achievable at a given distance between the tag and the reader.

sates this loss of SNR by increasing the symbol period to 10 \times , which in turn reduces the throughput.

To analyze the energy efficiency that BackFi link achieves for different combinations of throughput and range, we plot REPB as a function of throughput achieved for different ranges in Fig. 9. To read this graph, note that for every value of range we studied (0.5 m, 1 m, 2 m, 4 m, 5 m), we have a different curve (with a different color). Now for each particular range, we check what combinations of tag symbol rate, modulation and coding rates employed at the tag can be successfully decoded at the BackFi AP. For each throughput, we look up all combination that achieve it, and their REPB from Table. 7 and choose a minimum REPB and plot a point. All the points for that particular range are now joined by lines to show the feasible points for each range.

Fig. 9 shows that for a given range, throughput increases are obtained by either increasing the symbol switching rate, moving to a denser modulation or higher coding rate or some combination of all three. Each one of these increases energy consumption as expected, which leads to the step increases in REPB. Of course certain throughputs simply cannot be supported at a given range because the link's SNR is not strong enough to decode the data. The vertical line indicates the maximum throughput that can be achieved for a given distance between the tag and the BackFi's reader. Hence we see the curves stopping after a certain throughput for different ranges. Overall REPB lies between 0.5 to 3 for most combinations.

Next, we plot how REPB changes as a function of range assuming we want the same throughput. For this experiment we pick two throughputs, 1.25 Mbps and 5 Mbps, for which we want to optimize the communication link. For each value of range, we pick the combination of tag symbol rate, modulation and coding rate that can achieve those throughputs if there are any. Among the possible combinations we pick the one with the lowest REPB and plot it for that range. Fig. 10 shows the REPB as function of range for these two throughputs.

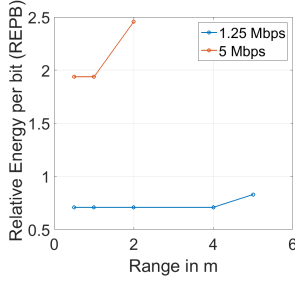


Figure 10: For achieving fixed throughput using BackFi for different distance, the tag needs to spend more energy as it goes far away. For achieving 1.25 Mbps we need to spend $2.5\times$ more than power needed for reference modulation, coding and switching rate.

Here we see expected results. For a fixed throughput, as we go to higher ranges we need to use lower coding rates. In our current design we only support two coding rates: 1/2 and 2/3. Hence for all these experiments we see the REPB change between two levels corresponding to the shift from higher coding rate to lower.

6.2 Reconstructing BackFi's performance

In this section, we aim to understand where do BackFi's benefits come from. As discussed before, BackFi's design has two key components: *self-interference cancellation* and *the decoding algorithm*. We try to shed light on the impact of each component on BackFi's performance.

Impact of self-interference cancellation: This component helps eliminate the unwanted leakage and environmental reflections from reducing the backscatter signal's SNR. Any uncanceled interference directly acts as noise to the backscatter signal and reduces throughput. To evaluate its impact we measure the SNR for the backscatter link at the reader and compare it to what the SNR would have been if cancellation was perfect. The experiment is conducted by placing the BackFi AP and the IoT sensor at 30 different locations in the testbed. For each location, we do ten runs where during each run we let the BackFi IoT sensor backscatter a known packet and measure the forward and backward channels from the tag using a vector network analyzer. In this scenario the VNA [42] acts as the BackFi AP and is being used so that we can measure the channels accurately for comparison. Next we perform the actual backscatter communication with a BackFi AP and decode the data after self-interference cancellation. We also compute the SNR of the demodulated phase modulated symbols from the tag and compare it to the SNR predicted by the channel measurement from the VNA. We plot these two SNR values for each run and each location as a scatter plot in Fig. 11(a). As we can see cancellation works well, the median degradation in SNR is less than 2.3 dB. This is consistent with earlier self-interference cancellation results from prior work [12, 11] which report a self-interference residue of 1.7 dB after cancellation.

Impact of Symbol Time and MRC: The second component of BackFi's decoder at the BackFi AP is the algorithm for dealing with the time-varying decoding problem. The algorithm has two key components: exploiting the larger symbol times from the tag packet to make an approximation that

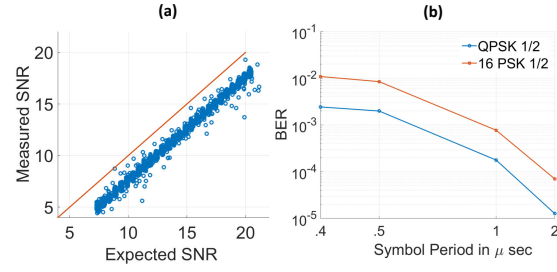


Figure 11: (a) Demonstrates the effect of imperfect cancellation on the degradation of the measured SNR vs the expected SNR at the reader of BackFi. When the cancellation is imperfect the environmental components are no longer completely removed and this acts as interference to the backscatter signal from the tag. (b) Demonstrates the diversity gains of MRC : as we increase the symbol time period, we have more samples for averaging, hence it improves the SNR. This increase in SNR results in lower bit error rate (BER) for a given modulation.

the channel can be converted into a simplified time invariant system and then apply MRC to solve it. MRC helps amplify the SNR of the signal by combining signal energy across time appropriately. Hence the key factor here is the tag symbol period which is inversely proportional to the tag symbol rate. To show the impact we plot the BER vs tag symbol rate for two modulations and a fixed coding rate of 1/2. The expectation is that as the tag symbol rate decreases and symbol time increases, the MRC gain will drive the BER down like a waterfall curve. Fig. 11(b) plots the BER as a function of decreasing tag symbol rate. As we can see, for this particular placement of AP and tag, at the highest tag symbol rate the BER is high between $10^{-2} - 10^{-3}$. As tag symbol rate decreases, the time diversity gain from MRC kicks in and BER drops down to between $10^{-4} - 10^{-5}$. This technique essentially points out the trade-off between throughput and range and why it exists.

6.3 Performance in typical WiFi Networks

BackFi tags only backscatter data when the WiFi reader is transmitting and they are activated by the reader with the activation sequence. The best candidate for the WiFi reader device is clearly the AP since it is likely the most dominant transmitter in a typical network. Nevertheless, in a typical network that is fully loaded (i.e. there is always outstanding traffic to transmit from the AP or a client), the AP will be transmitting a fraction of the time which would imply that the BackFi link would also be active for the same fraction. We evaluate the throughput BackFi can provide under such typical network conditions.

To conduct this experiment, we took traces from open source data [24, 47, 41]. The traces are captured for a wide variety of scenarios for heavily loaded networks. If an AP is not loaded and there is a lot of idle channel time, then a BackFi AP can initiate backscatter communication anyway by sending dummy packets just for that purpose. Hence the interesting case is when the network is loaded and backscatter opportunities are limited due to contention.

Next, we filter the traces to only contain AP transmissions and replay the collected trace using our WARP based BackFi AP implementation to simulate the same traffic conditions.

In other words, in our emulated experiment the WARP radio only transmits when the corresponding AP transmitted in the collected trace. We place a BackFi tag at a fixed distance of 2 m from the BackFi AP. We also activate the tag only at the times the AP is transmitting. We repeat this experiment for each AP we captured traces for, a total of 20 different APs. For each replay, we calculate the average throughput obtained by the BackFi link. Fig. 12(a) plots the CDF of these throughputs.

As we can see, in a loaded network, the BackFi link can obtain a median throughput of 4 Mbps. For a range of 2 m, the optimal throughput when the BackFi AP is continuously transmitting an excitation signal is 5 Mbps, hence this amounts 80% of the optimal throughput under realistic WiFi network conditions. The above number can be improved further if more WiFi devices have BackFi functionality. Specifically the above experiment assumed that only the AP has BackFi functionality. However if we can integrate the same into our laptops and smart-phones and turn them into gateways for BackFi links, then the BackFi link can be active for larger fractions of time.

6.4 Impact on the WiFi Network

A natural question is whether BackFi affects the performance of the WiFi network itself when the AP is doubling up as a WiFi backscatter reader. Specifically, one might imagine that the tags backscatter signals could propagate to the actual WiFi client which is the destination of the transmission from the AP and act as interference.

To quantify what impact one might see in a general WiFi network, we place the BackFi AP and ten clients at random locations in the testbed. Next we place the tag at increasing distances from the AP and calculate the WiFi throughput with and without an active BackFi tag. We repeat this experiment for 30 different configurations of the AP and the clients. We plot the throughputs with and without an active BackFi tag for different ranges between the BackFi AP and the tag in Fig. 12(b). The results confirm the previous benchmark, essentially when the tag and the AP reader are extremely close (between 0.25 – 0.5m), there is a small impact on network throughput of less than 10%. Otherwise the normal WiFi network performance is negligibly affected since the backscatter signals are so weak.

6.5 Micro-benchmark Impact on WiFi

We now evaluate the worst case scenario for the WiFi client. This corresponds to the case where the tag is very close to the AP (at a distance of 0.25m) because in this case the backscatter signals would be the strongest. Next we take a single WiFi client and place it at different distances so that we achieve each of the different rates of WiFi. Now for each WiFi bitrate, we evaluate the PHY layer throughput achieved with and without a BackFi tag being active. Fig. 13.a plots the CDF of WiFi throughputs achieved for this link with and without a BackFi tag active. As we can see, the effect is minimal. The only case where there is a noticeable difference is when the WiFi AP and the client are using the highest bitrate of 54 Mbps where small decreases in SNR (as shown

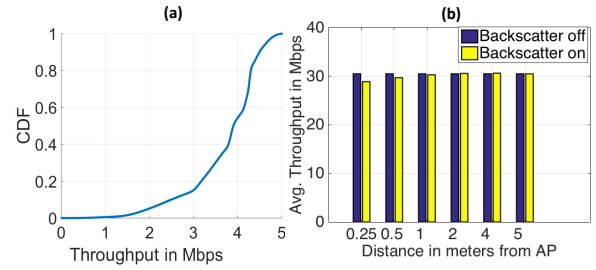


Figure 12: WiFi Deployments: (a) Throughput of BackFi's tag at a distance of 1m from the BackFi's reader under normal WiFi deployment. Note that BackFi tag is active only when the BackFi's reader is transmitting. Hence we achieve on an average 4 Mbps throughput vs the maximum throughput of 5Mbps. (b) Average throughput for all the clients at different locations as a function of distance of tag from the AP. As the tag moves away from the AP, it receives and radiates a smaller signal which will have smaller effect at the client. Hence, when the tag is at 0.25 m, we see a 10% throughput drop when tag is modulating. As the tag moves away from AP, we see no degradation in the average throughput.

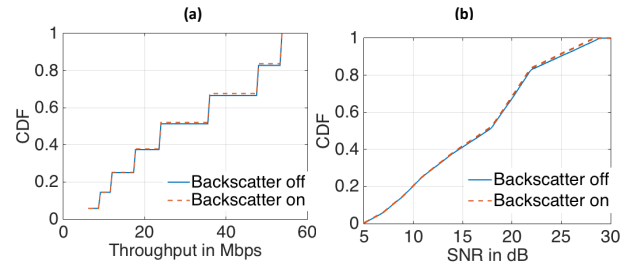


Figure 13: (a) Shows the CDF of the client throughput when the tag is placed at 0.25m from the AP. As seen, there is almost no degradation for lower bit rate of 6 Mbps, as client is farther from AP and the SNR required at the client to decode 6 Mbps is small. However, we observe noticeable difference at 54 Mbps, where both clients are closer to BackFi's AP and need higher SNR to decode data. (b) shows the degradation of SNR for tag on and tag off for each point for the plot on the left.

in Fig. 13.b) can force the WiFi AP to occasionally switch to lower bitrates.

7. CONCLUSION AND FUTURE WORK

BackFi provides a high throughput, sufficient range and a low power backscatter communication link using ambient WiFi signals. BackFi's range and throughput can be enhanced further with the use of multiple antennas at the WiFi APs since multiple antennas at the AP provides additional diversity combining gain. We can incorporate multiple antennas at the AP with minimal changes in BackFi's link layer protocol. Specifically, each transmit antenna would need a silent slot to eliminate the environmental component corresponding to that antenna. We could exploit existing WiFi MIMO packet structure for estimating the environment as it has preamble slots where only one transmit antenna is active. We can then perform MRC combining for the signals received across space from multiple antennas, providing BackFi with better SNR.

We believe, the combination of performance and piggybacking on existing signals demonstrated by BackFi can bring us closer to the vision of ubiquitous RF powered computing

and communication gadgets in the physical world. However, much work remains in realizing this vision, including designing protocols to manage a network of BackFi tags connected to an AP and designing techniques to figure out how to balance sensing, computing and communication needs within a constrained energy budget. This continues to be our future work.

Acknowledgments: We would like to thank Kun Tan, the anonymous reviewers, the Stanford Networked Systems Group members, and Pengyu Zhang for their insightful comments.

8. REFERENCES

- [1] *Analog Devices ADG904 RF SP4T*. http://www.analog.com/media/en/technical-documentation/data-sheets/ADG904_904R.pdf.
- [2] *Cypress Semiconductor CY62146EV30 SRAM*. <http://www.cypress.com/?docID=48695>.
- [3] *EPC Class-1 Gen-2 UHF RFID*. http://www.gs1.org/gsm/kc/epcglobal/uhfclg2/uhfclg2_1_2_0-standard-20080511.pdf.
- [4] *Improving whole home coverage and power efficiency*. <https://www.qualcomm.com/invention/research/projects/wi-fi-evolution/80211ah>.
- [5] *ThingMagic. Mercury6e rfid reader module*. <http://www.thingmagic.com/embedded-rfid-readers>.
- [6] *User Guide: KC705 Evaluation Board for the Kintex-7 FPGA*. http://www.xilinx.com/support/documentation/boards_and_kits/kc705/ug810_KC705_Eval_Bd.pdf.
- [7] *WARP Project*. <http://warpproject.org>.
- [8] E. Aryafar et. al. Midu: enabling mimo full duplex. In *ACM Mobicom '12*.
- [9] D. Bharadia, K. R. Joshi, and S. Katti. Full duplex backscatter. In *ACM HotNets'13*.
- [10] D. Bharadia and S. Katti. Fastforward: Fast and constructive full duplex relays. In *ACM SIGCOMM'14*.
- [11] D. Bharadia and S. Katti. Full duplex mimo radios. In *NSDI'14*.
- [12] D. Bharadia, E. McMillin, and S. Katti. Full duplex radios. In *ACM SIGCOMM'13*.
- [13] D. Brennan. Linear diversity combining techniques. *IEEE'03*.
- [14] M. Buettner, B. Greenstein, and D. Wetherall. Dewdrop: An energy-aware runtime for computational rfid. In *NSDI'11*.
- [15] M. Buettner and D. Wetherall. A software radio-based uhf rfid reader for phy/mac experimentation. In *IEEE RFID'2011*.
- [16] J. I. Choi et. al. Achieving single channel, full duplex wireless communication. In *MobiCom '10*.
- [17] M. Duarte, C. Dick, and A. Sabharwal. Experiment-driven characterization of full-duplex wireless systems. *CoRR*, abs/1107.1276, 2011.
- [18] M. Durante and S. Mahlke. An ultra low power wakeup receiver for wireless sensor nodes. In *SENSORCOMM '09*.
- [19] J. Ensworth and M. Reynolds. Every smart phone is a backscatter reader: Modulated backscatter compatibility with bluetooth 4.0 low energy (ble) devices. In *RFID IEEE, 2015*.
- [20] E. Everett, A. Sahai, and A. Sabharwal. Passive self-interference suppression for full-duplex infrastructure nodes. *CoRR*, abs/1302.2185, 2013.
- [21] K. Gudan et. al. Feasibility of wireless sensors using ambient 2.4ghz rf energy.
- [22] J. Gummesson et. al. On the limits of effective hybrid micro-energy harvesting on mobile crfd sensors. In *ACM MobiSys '10*.
- [23] J. Gummesson, P. Zhang, and D. Ganesan. Flit: A bulk transmission protocol for rfid-scale sensors. In *ACM MobiSys '12*.
- [24] A. Gupta, J. Min, and I. Rhee. Wifox: Scaling wifi performance for large audience environments. In *ACM CoNEXT '12*.
- [25] H. Ishizaki, H. Ikeda, Y. Yoshida, T. Maeda, T. Kuroda, and M. Mizuno. A battery-less wifi-ber modulated data transmitter with ambient radio-wave energy harvesting. In *VLSIC, 2011*.
- [26] M. Jain, J. I. Choi, T. Kim, D. Bharadia, S. Seth, K. Srinivasan, P. Levis, S. Katti, and P. Sinha. Practical, real-time, full duplex wireless. *MobiCom '11*.
- [27] B. Kellogg et. al. Wi-fi backscatter: Internet connectivity for rf-powered devices. In *ACM SIGCOMM '14*.
- [28] V. Liu, A. Parks, V. Talla, S. Gollakota, D. Wetherall, and J. R. Smith. Ambient backscatter: Wireless communication out of thin air. In *ACM SIGCOMM '13*.
- [29] C. Mikeka, H. Arai, A. Georgiadis, and A. Collado. Dtv band micropower rf energy-harvesting circuit architecture and performance analysis. In *RFID-TA IEEE 2011*.
- [30] P. Nikitin and K. Rao. Theory and measurement of backscattering from rfid tags. *Antennas and Propagation Magazine, IEEE'2006*.
- [31] S. Oh, N. Roberts, and D. Wentzloff. A 116nw multi-band wake-up receiver with 31-bit correlator and interference rejection. In *CICC, 2013 IEEE*.
- [32] U. Olgun, C.-C. Chen, and J. Volakis. Design of an efficient ambient wifi energy harvesting system. *IET 2012*.
- [33] A. Parks and J. Smith. Sifting through the airwaves: Efficient and scalable multiband rf harvesting. In *IEEE RFID 2014*,
- [34] A. N. Parks et. al. Turbocharging ambient backscatter communication. In *ACM SIGCOMM'14*.
- [35] S. Patel et. al. A review of wearable sensors and systems with application in rehabilitation. *Journal of neuroengineering and rehabilitation, 2012*.
- [36] N. Pletcher, S. Gambini, and J. Rabaey. A 52 micro w wake-up receiver with - 72 dbm sensitivity using an uncertain-if architecture. *Solid-State Circuits, IEEE 2009*.
- [37] N. Pletcher and J. M. Rabaey. *Ultra-Low Power Wake-Up Receivers for Wireless Sensor Networks*. PhD thesis, University of California, Berkeley, May 2008.
- [38] J. Proakis. *Digital Communications*. McGraw-Hill Series in Electrical and Computer Engineering. Computer Engineering. McGraw-Hill, 2001.
- [39] B. Radunovic, D. Gunawardena, P. Key, A. Proutiere, N. Singh, V. Balan, and G. Dejean. Rethinking indoor wireless mesh design: Low power, low frequency, full-duplex. In *WIMESH IEEE 2010*.
- [40] N. Roberts and D. Wentzloff. A 98nw wake-up radio for wireless body area networks. In *IEEE RFIC 2012*.
- [41] M. Rodrig, C. Reis, R. Mahajan, D. Wetherall, and J. Zahorjan. Measurement-based characterization of 802.11 in a hotspot setting. In *ACM SIGCOMM Workshop E-WIND '05*.
- [42] Rohde & Schwarz. *Vector Network Analyzer User Manual*.
- [43] A. Sahai, G. Patel, C. Dick, and A. Sabharwal. On the impact of phase noise on active cancellation in wireless full-duplex. *CoRR*, abs/1212.5462, 2012.
- [44] A. Sample and J. Smith. Experimental results with two wireless power transfer systems. In *IEEE RWS '09*.
- [45] A. Sample et. al. Design of a passively-powered, programmable sensing platform for uhf rfid systems. In *IEEE RFID, 2007*.
- [46] A. P. Sample et. al. *Wireless ambient radio power. In Wirelessly Powered Sensor Networks and Computational RFID*, pages 223–234. Springer, 2013.
- [47] A. Schulman, D. Levin, and N. Spring. On the fidelity of 802.11 packet traces. In *PAM'08*.
- [48] R. Shigetani et. al. Ambient rf energy harvesting sensor device with capacitor-leakage-aware duty cycle control. *IEEE Sensors Journal*.
- [49] S. Thomas and M. Reynolds. A 96 mbit/sec, 15.5 pj/bit 16-qam modulator for uhf backscatter communication. In *IEEE RFID 2012*.
- [50] J. Wang et. al. Efficient and reliable low-power backscatter networks. *SIGCOMM Commun. Rev. 2012*.
- [51] D. Yeager et. al. Wirelessly-charged uhf tags for sensor data collection. In *IEEE RFID 2008*.
- [52] H. Zhang et. al. Moo: A batteryless computational rfid and sensing platform. 2011.
- [53] J. Zhang et. al. Uwb systems for wireless sensor networks. *IEEE 2009*.
- [54] P. Zhang and D. Ganesan. Enabling bit-by-bit backscatter communication in severe energy harvesting environments. In *NSDI'14*.
- [55] P. Zhang et. al. Ekhonet: High speed ultra low-power backscatter for next generation sensors. In *ACM MobiCom '14*.